



DOCUMENTATION PAGE

Form Approved  
OMB No. 0704-0188

2

tion is estimated to average 1 hour per response, including the time for reviewing instructions, searching existing data sources, gathering and reviewing the collection of information. Send comments regarding this burden estimate or any other aspect of this collection of information, including this burden estimate, to Washington Headquarters Services, Directorate for Information Operations and Reports, 1215 Jefferson Avenue, Alexandria, VA 22304-4302, and to the Office of Management and Budget, Paperwork Reduction Project (0704-0188), Washington, DC 20503.

1. AGENCY USE ONLY (Leave blank)		2. REPORT DATE		3. REPORT TYPE AND DATES COVERED Reprint	
4. TITLE AND SUBTITLE Title shown on Reprint				5. FUNDING NUMBERS DAA403-91-C-0035	
6. AUTHOR(S) Author(s) listed on Reprint					
7. PERFORMING ORGANIZATION NAME(S) AND ADDRESS(ES) Scientific Research Associates, Inc. Hastonbury, CT 06033				8. PERFORMING ORGANIZATION REPORT NUMBER	
9. SPONSORING/MONITORING AGENCY NAME(S) AND ADDRESS(ES) U. S. Army Research Office P. O. Box 12211 Research Triangle Park, NC 27709-2211				10. SPONSORING/MONITORING AGENCY REPORT NUMBER ARO 28646.2-EL	
11. SUPPLEMENTARY NOTES The view, opinions and/or findings contained in this report are those of the author(s) and should not be construed as an official Department of the Army position, policy, or decision, unless so designated by other documentation.					
12a. DISTRIBUTION/AVAILABILITY STATEMENT Approved for public release; distribution unlimited.				12b. DISTRIBUTION CODE	
13. ABSTRACT (Maximum 200 words)  ABSTRACT ON REPRINT  DTIC SELECTE MAY 06 1993 S B D					
14. SUBJECT TERMS				15. NUMBER OF PAGES	
				16. PRICE CODE	
17. SECURITY CLASSIFICATION OF REPORT UNCLASSIFIED		18. SECURITY CLASSIFICATION OF THIS PAGE UNCLASSIFIED		19. SECURITY CLASSIFICATION OF ABSTRACT UNCLASSIFIED	
				20. LIMITATION OF ABSTRACT UL	

# Temperature description of transport in single- and multiple-barrier structures

H L Grubint, T R Govindant, B J Morrisont, D K Ferry† and M A Stroscio‡

†Scientific Research Associates, Inc. Glastonbury, CT 06033, USA

‡Arizona State University, Tempe, AZ 85287-6206, USA

§Army Research Office, Research Triangle Park, NC 27709-2211, USA

**Abstract.** Barrier calculations based upon solutions of the Liouville equation in the coordinate representation reveal a complicated spatial dependence of the quantum distribution function near and within the barriers. Within the framework of classical transport this spatial dependence suggests equilibrium electron temperature values that differ from the ambient. The prospect of quantum heating and cooling under equilibrium conditions is examined and dispelled in favour of an interpretation that includes density-gradient contributions.

## 1. Introduction

Calculations based upon solutions of the Liouville equation in a density matrix formulation yield a complicated spatial distribution with a mean kinetic energy in equilibrium that differs significantly from the classical result. In particular, where classical physics teaches that the energy per particle is  $k_B T/2$  per degree of freedom for a Boltzmann distribution, quantum physics, as pointed out by Wigner [1], teaches otherwise. The origin of this difference lies in the presence of quantum mechanical forces arising from gradients in density (Ancona and Iafrate, [2]), and are suggestive of a spatially dependent local temperature in both equilibrium and non-equilibrium cases, although spatial dependent carrier temperature in equilibrium introduces interpretive difficulties. To avoid this difficulty one either abandons the spatial-dependent temperature description, or retains it for non-equilibrium studies and seeks another description for equilibrium. But in either case, it is necessary to demonstrate its origin. This is provided below for equilibrium conditions.

## 2. Energy and temperature

Classical physics indicates that the mean kinetic energy in equilibrium for carriers obeying Boltzmann statistics is

$$\langle E \rangle = \frac{2}{(2\pi)^3} \int d^3p (p^2/2m) f(x, p) = \frac{3}{2} \rho k_B T \quad (1)$$

$\equiv \rho \epsilon$

where  $f(x, p)$  is the classical distribution function, and  $\epsilon$ , the mean kinetic energy per particle, is independent of

position, as is the consequent electron temperature. For quantum structures, in which quantum distribution functions are required,  $\epsilon$  is generally *spatially dependent* [1], and on the basis of equation (1) suggests a spatially dependent equilibrium carrier temperature. Because of the significance of carrier temperature in interpreting hot-carrier phenomena, the spatial dependence of the mean energy per particle, and the origin of this dependence is discussed through solutions to the Liouville equation

$$i\hbar \partial \rho_{op} / \partial t = [H, \rho_{op}] \quad (2)$$

which in the coordinate representation is a differential equation for  $\rho(x, x', t)$

$$\partial \rho / \partial t + (\hbar/2mi) (\nabla^2 - \nabla'^2) \rho - (1/i\hbar) [V(x, t) - V(x', t)] \rho = 0. \quad (3)$$

To expose the essential features of this discussion, we assume Boltzmann statistics, spatial variations only along the  $x$  direction, and free particle behaviour along the  $y$  and  $z$  directions. Transforming equation (3) to centre of mass and non-local coordinates,  $r = (x + x')/2$ ,  $\zeta = (x - x')/2$ ,  $\rho \Rightarrow \rho(r + \zeta, r - \zeta)$ , we find

$$\rho_r + (\hbar/2mi) \rho_{r\zeta} - (1/i\hbar) [V(r + \zeta, t) - V(r - \zeta, t)] \rho = 0. \quad (4)$$

In the above equation subscripts denote differentiation. The potential  $V$  in equations (3) and (4) is the sum of all heterostructure contributions,  $V_0(x)$ , and contributions from Poisson's equation:

$$\partial / \partial x [ \epsilon(x) \partial V_{sc} / \partial x ] = -e^2 [ \rho(x, x) - \rho_0(x) ] \quad (5)$$

where the subscript 'sc' denotes self-consistent;  $\rho_0(x)$  is the background 'jellium' doping distribution. The diagonal components of solutions to equation (4) (along the diagonal  $r = x$  and  $\zeta = 0$ ) provide the density, while the



8/15

expectation value of energy  $\langle E \rangle$  is obtained from the diagonal components of the kinetic energy density matrix [3]

$$E(r + \zeta, r - \zeta) = -\hbar^2/8m\rho_{\zeta\zeta}. \quad (6)$$

An approximate form of the expectation values of the density and the energy density [1, 4, 5] for one degree of freedom is:

$$\rho(x) = \rho(x, x) = \rho_0 \exp[-(V + Q/3)/k_B T] \quad (7)$$

$$E(x) = [(k_B T/2) + (\hbar^2/24mk_B T)V_{xx}]\rho(x). \quad (8)$$

In equation (7),  $\rho_0$  is a reference density, and  $Q(x)$  is the Bohm quantum potential (see, e.g., [6]):

$$Q(x) = -(\hbar^2/2m)(\rho^{1/2})_{xx}/\rho^{1/2}. \quad (9)$$

The second term of equation (8) is referred to as the Wigner contribution. In equilibrium the spatial dependence of the energy per particle,  $\varepsilon$ , as given by equation (8) is second order in  $\hbar$ . To this order, if the potential appearing in equation (8) is represented by the Boltzmann relation between density and potential energy,  $\rho(x) = \rho_0 \exp[-V(x)/k_B T]$ , it is seen that the spatial dependence of  $\varepsilon$  is a direct consequence of the spatial derivatives of density. In this context the origin of the quantum correction to  $\varepsilon$  is the same as the origin of the quantum potential.

### 3. Calculations

The spatial dependence of  $\varepsilon$  and the origin of the quantum contributions to transport arise from gradients in the carrier density. These features are illustrated through solutions to the Liouville equation for two equilibrium solutions using Maxwellian boundary condition as discussed in [7]. Two cases are considered. For the first calculation a single barrier characterized by a potential

$$V_0(x) = 300(\text{meV}) \exp[-(x/12.5 \text{ \AA})^2] \quad (10)$$

is placed within a uniform, 1500 \AA long, structure doped to  $10^{18} \text{ cm}^{-3}$ . The two-dimensional density matrix,  $\rho(x, x')$  as obtained from the Liouville and Poisson equations is displayed in figure 1(a). In equilibrium the density matrix is real and symmetric,  $\rho(x, x') = \rho(x', x)$ , and the solution is completely represented by one-half of the matrix on either side of the diagonal,  $x = x'$ , as displayed in figure 1(a). The charge density  $\rho(x) = \rho(x, x)$  is displayed as a line plot in figure 1(b), where since most of the structure in the solution is contained within a range of 250 \AA, about the centre, only 500 \AA of the results are displayed. Figure 1(b) displays a significant reduction of charge within the barrier, as well as charge accumulation on either side of the barrier. While the reduction of charge within the barrier is a consequence of the presence of the barrier, the excess charge adjacent to the barrier is a consequence of both self-consistency in the calculation and wavefunction (or density matrix) continuity across the barrier. The spatial dependence of the charge is

consistent with the condition of global charge neutrality. Figure 1(b) also displays two additional plots. The curve reaching the lowest value of density within the barrier is obtained from the classical Boltzmann relation between density and potential energy; the curve reaching intermediate values of density within the barrier is obtained from equation (7). Note that away from the barrier the density from equation (7) approaches a value that is less than the classical value, a result that is a consequence of a change in curvature of the potential as the boundaries are approached. Neither approximate solution can be regarded as an adequate representation of the complete solution, although the quantum-corrected solution possesses the general features of a density that is higher (than classical) within the barrier and lower (than classical) adjacent to the barrier. Figure 1(c) displays the potential distribution. The lowering of the potential adjacent to the barrier ( $\sim 20 \text{ meV}$ ) is a consequence of the excess charge and self-consistency. Figure 1(d) displays the quantum potential; note that its value is greater than  $-300 \text{ meV}$  in the centre of the barrier. The energy density matrix represents the curvature of the density matrix in the non-local direction. As seen in figure 1(a), the curvature is steeper where there is excess charge and changes sign within the barrier. The mean kinetic energy per particle,  $\varepsilon$ , obtained from the density matrix is displayed in figure 1(e), along with the Wigner contribution as obtained from equation (8). It is apparent that the main origin of the structure leading to the Wigner contribution is the quantum potential. The negative value of  $\varepsilon$  within the barrier and the positive excess value of energy adjacent to the barrier suggest that the Wigner contribution is not a correction, but represents a dominant effect, and that temperature concepts (which must include negative values) are not likely to be germane within the context of equilibrium transport.

The spatial dependence of the mean kinetic energy per particle is also of significance in multiple barrier structures. This is examined for a double barrier structure with

$$V_0(x) = (300 \text{ meV}) \{ \exp[-(x - 75 \text{ \AA})/12.5 \text{ \AA}]^2 + \exp[-(x + 75 \text{ \AA})/12.5 \text{ \AA}]^2 \} \quad (11)$$

The barriers are centrally placed within a 1500 \AA  $n^+ n^- n^+$  structure with adjacent  $10^{18} \text{ cm}^{-3} n^+$  regions, and a centrally placed 500 \AA,  $10^{15} \text{ cm}^{-3}$  region. The two-dimensional density matrix is displayed in figure 2(a), obtained from the Liouville and Poisson equations. There is excess charge between the barriers, a modest increase in curvature between the barriers and a change in sign of the curvature within the barriers. The line plot of density is shown in figure 2(b) over a reduced range of 600 \AA. The density as obtained from equation (7) displays a significantly lower charge density within the barrier but *order of magnitude agreement within the quantum well*. The classical solution for density is completely unacceptable. The potential distribution, shown in figure 2(c), reaches flat-band beyond 400 \AA on either side of the

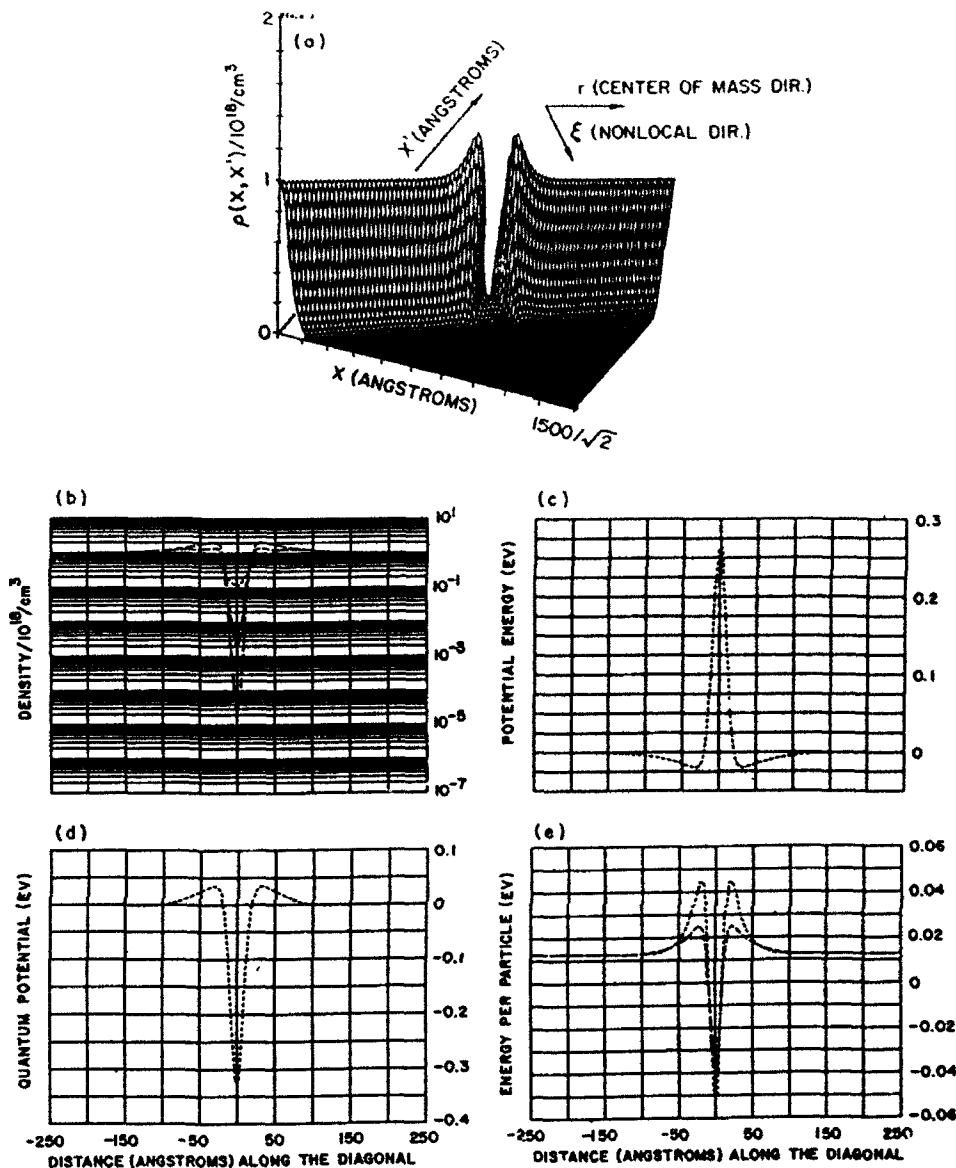


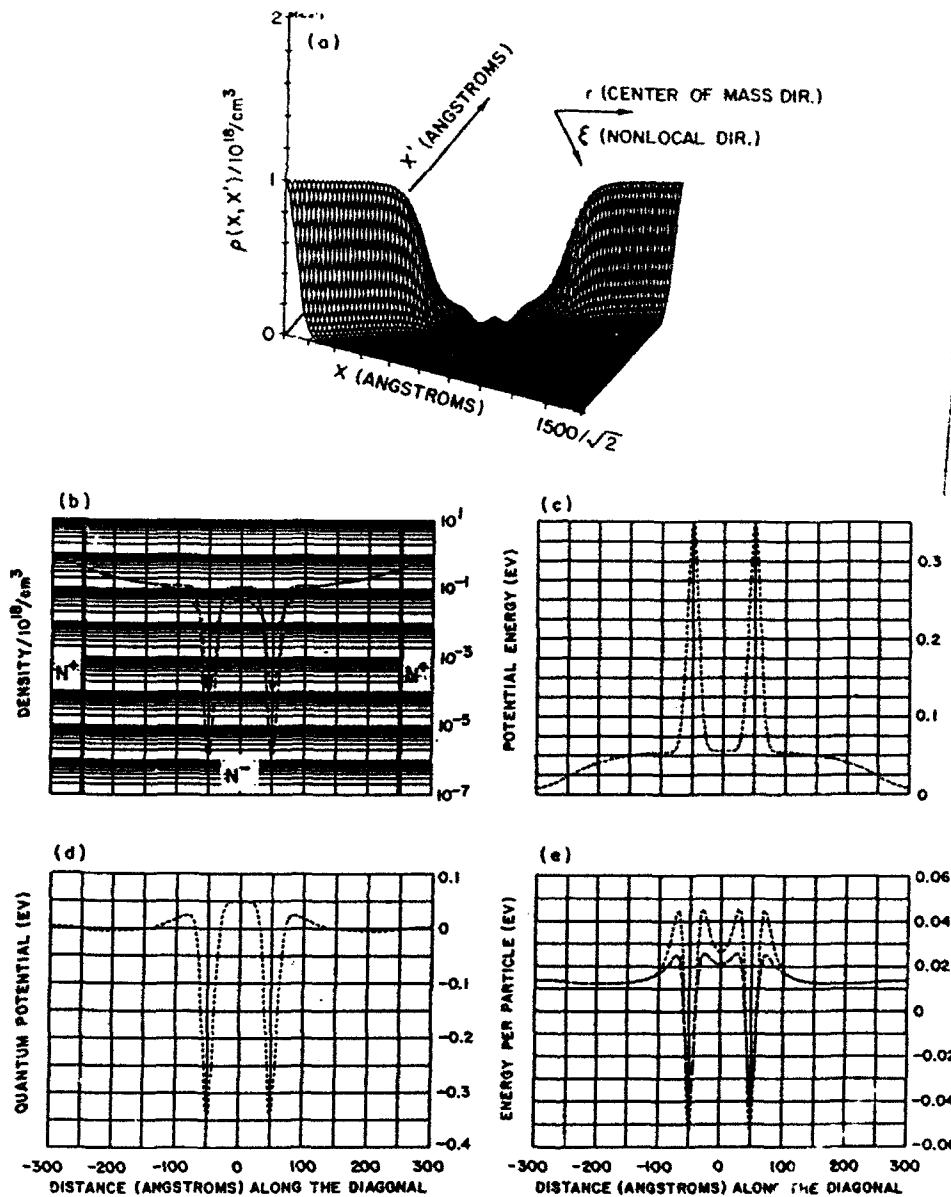
Figure 1. (a) Density matrix for a single-barrier structure. The physical dimension of the structure is  $1500 \text{ \AA}$ , requiring that the density matrix, which is calculated over a square matrix, is of side  $1500 \text{ \AA}/\sqrt{2}$ . The centre of mass and non-local directions are indicated; (b) diagonal component of the density matrix (---), from equation (7) (---), classical relation (—); (c) potential energy  $V(x)$ ; (d) quantum potential; (e) energy per particle from density matrix (---), from equation (8) (—).

origin; its increase arises from self-consistency and the reduction of charge in the low-doped region compared with the bounding charge density. The quantum potential displayed in figure 2(d) is positive within the quantum well, and emphasizes the reduction in charge density compared with the classical value; it is negative within the barriers, as in the case of the single-barrier structure, and positive outside of the barriers. The positive value outside of the barriers is a consequence of wavefunction and density matrix continuity within the classically accessible region. Note again that the structure of the quantum potential is apparently the main origin of the structure leading to the Wigner contribution to the

energy per particle, as seen in figure 2(e). As in the case of the single barrier of figure 1 the calculations suggest that the Wigner contribution is not a correction but represents a dominant effect, and that temperature concepts are not germane in the context of equilibrium transport.

#### 4. Conclusions

The calculations of figures 1 and 2 reveal significant spatial variations in energy associated with density gradients. Mathematically, these energy variations, which are a consequence of wavefunction continuity as repre-



Accession For	
ERIC Search	<input checked="" type="checkbox"/>
DTIC TAB	<input type="checkbox"/>
Unannounced	<input type="checkbox"/>
Justification	<input type="checkbox"/>
By _____	
Dist. _____	
Availability Codes	
Dist	Avail and/or Special
A-1	20

DTIC QUALITY INSPECTED

Figure 2. (a) Density matrix for a double-barrier structure; (b) diagonal component of the density matrix (---), from equation (7) (---), classical relation (—); (c) potential energy  $V(x)$ ; (d) quantum potential; (e) energy per particle from density matrix (---), from equation (8) (---).

sented by 'curvature' in the density matrix, are suggestive of quantum heating and/or cooling. Physically these energy variations represent the influence of local quantum mechanical density dependent forces on the carriers. While their magnitudes indicate that they must be accounted for in all quantum mechanical treatments of transport in mesoscopic structures, an interpretation in terms of heating or cooling in equilibrium is problematic.

**Acknowledgement**

This work was supported by ARO and ONR (HLG, TRG, DKF) and AFOSR (HLG, TRG and BJM).

**References**

- [1] Wigner E P 1932 *Phys. Rev.* **40** 749
- [2] Ancona M A and Iafrate G J 1989 *Phys. Rev.* **B39** 9536
- [3] Grubin H L, Govindan T R and Strosio M A to be published
- [4] Grubin H L and Kreskovsky J P 1989 *Solid-State Electron.* **32** 1071
- [5] Wollard D L, Strosio M A, Littlejohn M A, Trew R J and Grubin H L 1991 *Proc. Workshop on Computational Electronics*, (Deventer: Kluwer) p 59
- [6] Philippidis C, Bohm D and Kaye R D 1982 *Nuovo Cimento* **B71** 75
- [7] Govindan T R, Grubin H L and deJong F J 1991 *NASECODE Conference*